On the Cramer-Rao lower Bound and the performance of synchronizers for (turbo) encoded systems

N. Noels[1], H. Steendam and M. Moeneclaey
TELIN department, Ghent University, St-Pietersnieuwstraat 4, 9000 Gent, Belgium
Email: {nnoels, hs, mm}@telin.UGent.be

***Abstract* - In this paper we derive the Cramer-Rao bound (CRB) for joint estimation of carrier phase, carrier frequency and timing from a noisy linearly modulated signal with *coded* data symbols. We obtain a closed-form expression for the CRB in terms of the marginal a posteriori probabilities of the coded symbols, allowing efficient numerical evaluation of the bound. We find that at low SNR, the CRB for coded transmission is considerably smaller than the CRB for uncoded transmission. We show that practical synchronizers that make clever use of the code properties yield a mean-square estimation error that is close to the CRB for coded transmission.**

I. Introduction

A common approach to judge the performance of parameter estimators consists of comparing their resulting mean-square estimation error (MSEE) to the Cramer-Rao bound (CRB), which is a fundamental lower bound on the error variance of unbiased estimators [1]. In order to avoid the computational complexity related to the *true* CRB, a *modified* CRB (MCRB) has been derived in [2] and [3]. The MCRB is much simpler to evaluate than the true CRB, but is in general looser (i.e. lower) than the CRB, especially at lower SNR. The CRB for the estimation of the carrier phase, the carrier frequency and the timing delay from *uncoded* data symbols has been obtained in [4]-[7]. In [8], the CRB for carrier phase estimation from *coded* data has been expressed in terms of the marginal a posteriori probabilities (APPs) of the coded symbols, allowing the numerical evaluation of the bound for a wide range of coded systems, including schemes with iterative detection.

In this contribution we consider the CRB for *joint* carrier phase, carrier frequency offset and timing recovery in *coded* systems. The bound is compared to (i) the MCRB, (ii) the CRB for uncoded transmission and (iii) the performance of practical synchronizers.

II. Problem Formulation

Let us consider the complex baseband representation r(t) of a noisy linearly modulated signal :

$$r(t) = \sum_{k=-K}^{K} a_k h(t - kT - \tau) \exp\big(j(\theta + 2\pi F t) \big) + w(t) \qquad (1)$$

where $\mathbf{a}=(a_{-K}, \ldots a_K)$ is a vector of L=2K+1 symbols taken from an M-PSK, M-QAM or M-PAM constellation according to a combination of an encoding rule and a mapping rule; h(t) is a *real-valued* unit-energy square-root Nyquist pulse; τ is the time delay, θ is the carrier phase at t=0, F is the carrier frequency offset; T is the symbol interval; w(t) is complex-valued zero-mean Gaussian noise with independent real and imaginary parts, each having a normalized power spectral density of $N_0/(2E_s)$, with E_s and N_0 denoting the symbol energy and the noise power spectral density, respectively.

Suppose that one is able to produce from an observation vector $\mathbf{r}$ an *unbiased* estimate $\hat{\mathbf{u}}$ of a deterministic vector parameter $\mathbf{u}$. Then the estimation error variance is lower bounded by the CRB [1]: $E_{\mathbf{r}}[(\hat{u}_i - u_i)^2] \geq CRB_i(\mathbf{u})$, where $CRB_i(\mathbf{u})$ is the i-th diagonal element of the inverse of the *Fisher information matrix* (FIM) $\mathbf{J}(\mathbf{u})$. The (i,j)-th element of $\mathbf{J}(\mathbf{u})$ is given by

$$\mathbf{J}_{ij}(\mathbf{u}) = E_{\mathbf{r}}\left[\frac{\partial}{\partial u_i} \ln(p(\mathbf{r};\mathbf{u})) \frac{\partial}{\partial u_j} \ln(p(\mathbf{r};\mathbf{u})) \right] \qquad (2)$$

Note that $\mathbf{J}(\mathbf{u})$ is a symmetrical matrix. When the element $\mathbf{J}_{ij}(\mathbf{u})=0$, the parameters u_i and u_j are said to be *decoupled*. The probability density $p(\mathbf{r};\mathbf{u})$ of $\mathbf{r}$, corresponding to a given value of $\mathbf{u}$, is called the *likelihood function* of $\mathbf{u}$, while $\ln(p(\mathbf{r};\mathbf{u}))$ is the *log-likelihood function* of $\mathbf{u}$. The expectation $E_{\mathbf{r}}[.]$ in (2) is with respect to $p(\mathbf{r};\mathbf{u})$. When the observation $\mathbf{r}$ depends not only on the parameter $\mathbf{u}$ to be estimated but also on a nuisance vector parameter $\mathbf{v}$, the likelihood function of $\mathbf{u}$ is obtained by averaging the likelihood function $p(\mathbf{r}|\mathbf{v};\mathbf{u})$ of the vector $(\mathbf{u},\mathbf{v})$ over the a priori distribution of the nuisance parameter: $p(\mathbf{r};\mathbf{u}) = E_{\mathbf{v}}[p(\mathbf{r} \mid \mathbf{v};\mathbf{u})]$. We refer to $p(\mathbf{r}|\mathbf{v};\mathbf{u})$ as the *joint* likelihood function, as $p(\mathbf{r}|\mathbf{v};\mathbf{u})$ is relevant to the joint estimation of $\mathbf{u}$ and $\mathbf{v}$.

As the evaluation of the expectations involved in $\mathbf{J}(\mathbf{u})$ and $p(\mathbf{r};\mathbf{u})$ is quite tedious, a simpler lower bound, called the modified CRB (MCRB), has been derived in [2] and [3]. The MCRB for joint carrier phase, carrier frequency offset and timing estimation, corresponding to r(t) from (1), is given by

$$E[(\hat{\theta} - \theta)^2] \geq MCRB_\theta = \frac{N_0}{2E_s L} \qquad (3)$$

[1] This work was supported by the InteruniversityAttraction Poles Programme P5/11 – Belgian Science Policy

$$E[(\hat{F}-F)^2 \cdot T^2] \geq MCRB_F = \frac{3N_0}{2\pi^2 E_s L (L^2-1)} \tag{4}$$

$$E[(\hat{\tau}-\tau)^2 / T^2] \geq MCRB_\tau = \frac{N_0}{2E_s L C_1} \tag{5}$$

where

$$C_1 = T^2 \int \left(\dot{h}(t)\right)^2 dt \tag{6}$$

The MCRB is much simpler to evaluate than the true CRB, but is in general looser than the CRB, i.e., $E_{\mathbf{r}}[(\hat{u}_i - u_i)^2] \geq CRB_i(\mathbf{u}) \geq MCRB_i(\mathbf{u})$. In [9], the high-SNR limit of the true CRB related to the estimation of a scalar parameter has been evaluated analytically and has been shown to coincide with the MCRB from (3)-(5).

III. Evaluation Of The CRB

A. CRB in terms of the marginal APPs of the coded symbols

With $\mathbf{u}=(\theta,F,\tau)$ and $\mathbf{v}=\mathbf{a}$, the joint likelihood function $p(\mathbf{r}|\mathbf{a};\theta,F,\tau)$ is, within a factor not depending on $(\theta,F,\tau,\mathbf{a})$, given by

$$p(\mathbf{r} \mid \mathbf{a};\theta,F,\tau) = \prod_{k=-K}^{K} F\left(a_k, \tilde{z}_k(\theta,F,\tau)\right) \tag{7}$$

where

$$F\left(a_k, \tilde{z}_k(\theta,F,\tau)\right) = \exp\left(\frac{E_s}{N_0}\left(2\,\mathrm{Re}\left[a_k^* \tilde{z}_k(\theta,F,\tau)\right] - |a_k|^2\right)\right) \tag{8}$$

In (7), $\mathbf{r}$ is a vector representation of the signal r(t) from (1), and $\tilde{z}_k(\theta,F,\tau) = z_k(F,\tau)e^{-j\theta}$, where $z_k(F,\tau)$ is defined as

$$z_k(F,\tau) = \int e^{-j2\pi F t} r(t) h(t - kT - \tau)\, dt \tag{9}$$

Hence, $\tilde{z}_k$ is a function of (θ,F,τ), whereas z_k depends only on (F,τ). For the log-likelihood function $\ln(p(\mathbf{r};\theta,F,\tau))$ we obtain

$$\ln p(\mathbf{r};\theta,F,\tau) = \ln\left(\sum_{i=0}^{M^L-1} \Pr[\mathbf{a}=\mathbf{c}_i]\, p(\mathbf{r} \mid \mathbf{c}_i;\theta,F,\tau)\right) \tag{10}$$

where $p(\mathbf{r}|\mathbf{c}_i,\theta,F,\tau)$ is given by (7) and i enumerates all M^L symbol sequences $\mathbf{c}_i$ of length L. Differentiation of (10) yields

$$\frac{\partial}{\partial u_\ell} \ln\left(p(\mathbf{r};\theta,F,\tau)\right) = \sum_{i=0}^{M^L-1} \frac{\Pr[\mathbf{a}=\mathbf{c}_i]\, p(\mathbf{r}|\mathbf{c}_i;\theta,F,\tau)}{p(\mathbf{r};\theta,F,\tau)} \frac{\partial}{\partial u_\ell} \ln\left(p(\mathbf{r}|\mathbf{c}_i;\theta,F,\tau)\right) \tag{11}$$

Made use of Bayes' rule, i.e.,

$$\frac{\Pr[\mathbf{a}=\mathbf{c}_i]\, p(\mathbf{r} \mid \mathbf{c}_i;\theta,F,\tau)}{p(\mathbf{r};\theta,F,\tau)} = \Pr[\mathbf{a}=\mathbf{c}_i \mid \mathbf{r};\theta,F,\tau] \tag{12}$$

and of (7), (11) is transformed into

$$\begin{aligned}\frac{\partial}{\partial u_\ell} \ln\left(p(\mathbf{r};\theta,F,\tau)\right) &= 2\frac{E_s}{N_0} E_{\mathbf{a}|\mathbf{r}}\left[\sum_{k=-K}^{K} \mathrm{Re}\left(a_k^* \tilde{z}_{\ell,k}\right)\right] \\ &= 2\frac{E_s}{N_0} \sum_{k=-K}^{K} E_{a_k|\mathbf{r}}\left[\mathrm{Re}\left(a_k^* \tilde{z}_{\ell,k}\right)\right] \\ &= 2\frac{E_s}{N_0} \sum_{k=-K}^{K} \sum_{m=0}^{M-1} \mathrm{Re}\left[H\left(\alpha_m, a_k, \tilde{z}_{\ell,k}, \tilde{\mathbf{z}}\right)\right]\end{aligned} \tag{13}$$

where

$$H\left(\alpha_m, a_k, \tilde{z}_{\ell,k}, \tilde{\mathbf{z}}\right) = \Pr[a_k = \alpha_m \mid \mathbf{r};\theta,F,\tau]\, \alpha_m^* \tilde{z}_{\ell,k} \tag{14}$$

$E_{\mathbf{a}|\mathbf{r}}[.]$ and $E_{a_k|\mathbf{r}}[.]$ refer to averaging over $\Pr[\mathbf{a}=\mathbf{c}_i \mid \mathbf{r};\theta,F,\tau]$ and $\Pr[a_k=\alpha_m \mid \mathbf{r};\theta,F,\tau]$, respectively, $(\alpha_0, \alpha_1, ..., \alpha_{M-1})$ denotes the set of constellation points, $\tilde{\mathbf{z}} = [\tilde{z}_{-K}, \ldots, \tilde{z}_K]^T$, and the subscript ℓ denotes differentiation with respect to u_ℓ, i.e., $\tilde{z}_{\ell,k} = \frac{\partial}{\partial u_\ell}(\tilde{z}_k)$ with $(u_1,u_2,u_3)=(\theta,F,\tau)$. No approximation is involved in obtaining (13). Substitution of (13) into (2) yields an exact expression of the FIM in terms of the *marginal* APPs $\Pr[a_k = \alpha_m \mid \mathbf{r};\theta,F,\tau]$ of the coded data symbols.

Taking (13) into account, the elements $J_{\ell\ell'}$ of the FIM from (2) can be represented as

$$J_{\ell\ell'} = 4\left(\frac{E_s}{N_0}\right)^2 \sum_{k_1,k_2=-K}^{K} \sum_{m_1,m_2=0}^{M-1} E\left[\begin{array}{l}\mathrm{Re}\left[H\left(\alpha_{m_1}, a_{k_1}, \tilde{z}_{\ell,k_1}, \tilde{\mathbf{z}}\right)\right] \\ \cdot \mathrm{Re}\left[H\left(\alpha_{m_2}, a_{k_2}, \tilde{z}_{\ell',k_2}, \tilde{\mathbf{z}}\right)\right]\end{array}\right] \tag{15}$$

where E[.] denotes averaging over the quantities $\tilde{\mathbf{z}}$, $\tilde{z}_{\ell,k_1}$ and $\tilde{z}_{\ell',k_2}$, whose statistics do not depend upon (θ,F,τ). Taking into account the Gaussian nature of the noise components in $\tilde{z}_k$ and $\tilde{z}_{\ell,k}$ we were able to perform *analytically* the averaging in (15) over $\tilde{z}_{\ell,k_1}$ and $\tilde{z}_{\ell',k_2}$, conditioned on $\tilde{\mathbf{z}}$ (as in [7]). Further evaluation of (15) then requires *numerical* averaging only over $\tilde{\mathbf{z}}$**.** The latter can be easily evaluated by numerical integration or Monte Carlo simulation over $\tilde{\mathbf{z}} = \{\tilde{z}_k\} = \{a_k + n_k\}$, where $\{a_k\}$ are data symbols taken from the constellation according

to the combination of the encoding rule and the mapping rule and $\{n_k\}$ are independent zero-mean complex Gaussian noise variables with variance equal to N_0/E_s.

We obtain that J_{12}, J_{22} and J_{23} are functions of the parameter τ. This implies that the CRB depends on the exact value of the unknown but deterministic time delay $\tau \in [-T/2, T/2]$ that is being estimated. However, under the usual assumption that the observation interval is much longer than the symbol duration (L>>1), this dependence can be safely ignored; this is confirmed by the numerical results (not reported here) for different values of τ. A similar quasi-independence (on τ) of the MCRB was pointed out in [3]. Inversion of the FIM (15) finally yields the CRB.

B. Evaluation of the marginal APPs of the coded symbols

In principle, any marginal APP $\Pr[a_k = \alpha_m | \mathbf{r}; \theta]$ can be obtained as a summation of joint APPs $\Pr[\mathbf{a} = \mathbf{c_i} | \mathbf{r}; \theta]$, which in turn can be computed from (12). However, the computational complexity of this procedure increases exponentially with the sequence length L.

For codes that are described by means of a trellis, the marginal APPs can be determined directly by means of the Bahl-Cocke-Jelinek-Raviv (BCJR) algorithm [10]. As its computational complexity grows only linearly with the number of states and with the sequence length L, the BCJR algorithm is the appropriate tool for marginal APP computation in case of linear block codes, convolutional codes and trellis codes, provided that the number of states is manageable.

When the coded symbol sequence results from the (serial or parallel) concatenation of two encoders that are separated by an interleaver (such as turbo codes [11]), the underlying overall trellis has a number of states that grows exponentially with the interleaver size. However, when the encoders themselves are described by a small trellis, the marginal APPs are computed by means of iterated application of the BCJR algorithm to the individual trellises, with exchange of extrinsic information between the BCJR algorithms at each iteration (the same computation is carried out when performing iterated turbo decoding instead of the too complex MAP symbol decoding). When the coded bits (conditioned on **r** and (θ,F,τ)) can be considered as independent (which is a reasonable assumption when the interleaver size is large), this iterative procedure yields the correct marginal APPs when reaching the steady state [12]. This approach is easily extended to other systems that use iterative decoding.

IV. Numerical Results And Discussion

Simulation results are obtained for the observation of L=1001 QPSK turbo-encoded symbols. The transmit pulse is a square-root cosine roll-off pulse with an excess bandwidth of either 20% or 100%. The turbo encoder consists of the parallel concatenation of two identical recursive systematic rate 1/2 convolutional codes with generator polynomials $(37)_8$ and $(21)_8$, through a pseudo random interleaver of length L; the output of the turbo encoder is punctured to obtain an overall rate of 1/2, and Gray mapped onto the QPSK constellation.

Our results indicate that the CRB for joint phase, frequency and timing estimation is essentially the same as the CRB for the estimation of a single parameter assuming the other parameters to be a priori known. There is almost no coupling between the parameters θ, F and τ, meaning that (at least for small errors) the inaccuracy in one parameter estimate does not impact the estimation of the other parameters.

In Fig. 1 we have plotted the ratio CRB/MCRB as a function of E_s/N_0 per coded symbol (solid curves). The result for uncoded transmission (UC) is also displayed (dashed curves). The considered E_s/N_0-range covers the normal operating range of the turbo receiver (1dB-2dB). We observe that the CRB is considerably smaller for coded transmission than for uncoded transmission. This indicates that it is potentially more accurate to estimate the synchronizer parameters from coded data than from uncoded data. As the mean square estimated error (MSEE) of synchronizers that do not exploit the code properties in the estimation process ('code-unaware' synchronizers) is lower bounded by the CRB for uncoded transmission (which we denote as $CRB_{uncoded}$), 'code-aware' synchronizers are potentially more accurate than 'code-unaware' synchronizers. The ratio $CRB_{uncoded}/CRB$ indicates to what extent synchronizer performance can be improved by making clever use of the code structure. At high SNR the CRB converges to the MCRB.

V. Actual Estimator Performance

In this section we consider the MSEE resulting from some joint phase and frequency estimators operating on the rate ½ turbo-encoded QPSK scheme from the previous section. The MSEE is compared to the CRB and the $CRB_{uncoded}$. The joint estimation of carrier phase and frequency is only marginally affected by a small timing estimation error (because (θ,F) and τ are essentially decoupled); therefore we have determined the mean square phase and frequency error assuming the timing to be known. Two scenarios are considered: A) carrier synchronization independent of turbo decoding and B) joint carrier synchronization and turbo decoding. The latter approach will be referred to as *turbo synchronization* in the sequel. For both scenarios, the MSEE for phase (Fig. 2) and frequency (Fig. 3) estimation was obtained as a function of the SNR. An observation of L=1001 (i.e. block size of the code) unknown data symbols was considered. A preamble of N known pilot symbols (PS) may be added at the beginning of each block to aid synchronization. A minimum of 10000 trials has been run; at each trial a new phase offset θ and a new frequency offset FT are taken from a uniform distribution over $[-\pi,\pi]$ and [-0.1,0.1], respectively. The phase error is measured modulo 2π and supported in the interval $[-\pi,\pi]$, except for the Non-Data-Aided (NDA) estimator. The phase error of the NDA estimator was measured modulo $\pi/2$, i.e. in the interval

[-π/4, π/4], as the NDA estimator for QPSK gives a 4-fold phase ambiguity.

A. Carrier synchronization independent of turbo decoding

For the synchronization scenario A, we implement the conventional NDA carrier synchronization scheme proposed in [13] for operation at very low values of E_s/N_0. This algorithm was originally developed for uncoded sequences and does not exploit the code structure; as a result its performance is lower bounded by the $CRB_{uncoded}$ (with $CRB_{uncoded} \geq CRB$).

The dashed curve in Figs. 2 and 3 corresponds to the MSEE for carrier phase and frequency estimation, respectively, as obtained with the NDA estimator. We observe that, with the chosen parameter values, the NDA estimator does not function properly at the normal (low) operating SNR of the code (1dB-2dB). The SNR threshold for frequency estimation from an observation of L=1001 symbols (see [14]) is located at about 3.5 dB. For $E_s/N_0 \geq 3.5$ dB, the algorithm achieves near optimal $CRB_{uncoded}$ performance, but for $E_s/N_0 < 3.5$ dB, the performance dramatically deteriorates across a narrow SNR interval.

The SNR threshold can be decreased by increasing the observation length L [14] (in [13], L=8192). However, if enlarging the observation interval is not an option, the combined Data-Aided (DA) and NDA frequency estimation approach proposed in [15] may be applied to soften the threshold. This approach consists of a two stage coarse-fine search. The DA estimator is used to coarsely locate the frequency offset, and then the more accurate NDA estimator attempts to improve the estimate within the uncertainty of the coarse estimator. After frequency and phase correction, the samples of the preamble are compared to the original pilot symbols and, if necessary, an extra multiple of π/2 is compensated for. In Figs. 2 and 3, the square markers illustrate the MSEE for carrier phase and frequency, respectively, as obtained with this DA-NDA estimator assuming the initial DA estimate is based on the observation of N preamble symbols. Results are displayed for N=128 and N=256. A threshold is still evident, but the performance below the SNR threshold degrades less rapidly. The more PS are used, the more the threshold softens. Relatively large preambles are required for the DA-NDA estimator to performs closely to the $CRB_{uncoded}$, e.g. with N=256 the overhead N/(N+L) equals about 20%.

B. Joint carrier synchronization and turbo-decoding

For the turbo synchronization scenario B, we implement the joint carrier synchronization and turbo-decoding scheme proposed in [16], which we further refer to as soft-Decision-Directed (sDD) estimator. As motivated in [16], it involves a practical implementation of the maximum likelihood (ML) estimator by means of the expectation-maximization (EM) algorithm. This algorithm converges iteratively to the ML estimate provided that the initial estimate is sufficiently accurate [17]. In our simulations we assume that the sDD estimator is initialized with a DA estimate obtained from a preamble of N consecutive PS, or with a combined DA-NDA estimate as described in subsection V.A. We will refer to these synchronization schemes as DA-sDD and DA-NDA-sDD, respectively. We assume that the PS are strictly used for the DA initialization, and that the (NDA-)sDD algorithm uses only the L coded symbols, so that the CRB derived in section III is indeed a valid lower bound on the overall performance of the algorithms. The synchronization process is completely integrated into the turbo detection system; at every turbo-decoder iteration, one EM iteration is performed. The sDD estimator takes advantage of the code properties; therefore its performance is lower bounded by, and should be compared to, the new CRB for coded transmission. The curves marked with triangles in Figs. 2 and 3 show the MSEE for carrier phase and frequency, respectively, as obtained with the DA-sDD estimator after 10 iterations of the turbo decoder/estimator and for N=256 and N=512 preamble symbols. With N=512, the DA-sDD estimator performs very closely to the new CRB. However, the resulting overhead of about 34% is often not acceptable. For N=256, the DA-sDD estimator performs worse than the DA-NDA estimator, except at high SNR (>4.5 dB). The curves marked with circles in Figs. 2 and 3 show the MSEE for carrier phase and frequency, respectively, as obtained with the DA-NDA-sDD estimator after 10 iterations of the turbo decoder/estimator and for N=128 and N=256 preamble symbols. Our results show that the DA-NDA-sDD estimator provides a considerable improvement over the DA-NDA estimator within the useful SNR range of the code, and meets the new CRB for coded transmission at values of SNR larger than about 1.5 dB for N=256 (about 20% overhead) and 2 dB for N=128 (about 11% overhead). This indicates the importance of an accurate initial estimate.

For the sake of completeness, we mention that a more sophisticated distribution of the PS across the burst may reduce the number of PS required to obtain a certain DA estimation accuracy, thereby increasing the spectral efficiency of the transmission system [15],[18].

VI. Conclusion

This contribution compares the CRB for joint carrier phase, carrier frequency offset and timing delay estimation in coded systems against the MCRB for transmission of a sequence of known training symbols and the $CRB_{uncoded}$ for uncoded transmission. We have found that the synchronizer parameters are essentially decoupled. This implies that (at least for small errors) the estimation inaccuracy for one parameter does not impact the estimation of the other parameters. It was shown that, at the normal operating SNR of the code, the CRB is much less than the $CRB_{uncoded}$. The $CRB_{uncoded}$ is a lower bound on the performance of synchronizers that make no use of the code structure. This implies that in order to approach optimal performance, estimators should make clever use of the code properties during the estimation process. The advantage of code-aware carrier recovery was illustrated with examples

of joint carrier phase and frequency estimation techniques available in the literature. The turbo synchronizer presented in [16], which is code-aware and performs joint carrier synchronization and turbo detection, has been shown to operate very closely to the CRB provided that a sufficiently accurate initial estimate is available. For timing recovery, no performance results have been presented. However, it has been shown in [19] that applying the turbo synchronization approach to timing estimation results in a very low MSEE, which is close to the new CRB for timing estimation from section III.

REFERENCES

[1] H.L. Van Trees, Detection, Estimation and Modulation Theory, New York: Wiley, 1968

[2] A.N. D'Andrea, U. Mengali and R. Reggiannini, "The modified Cramer-Rao bound and its applications to synchronization problems," IEEE Trans. Comm., vol COM-24, pp. 1391-1399, Feb.,Mar.,Apr. 1994.

[3] F. Gini, R. Reggiannini and U. Mengali, "The modified Cramer-Rao bound in vector parameter estimation," IEEE Trans. Commun., vol. CON-46, pp. 52-60, Jan. 1998

[4] W.G. Cowley, "Phase and Fequency estimation for PSK packets: bounds and algorithms," IEEE Trans. Comm., vol COM-44, pp. 26-28, Jan. 1996.

[5] F. Rice, B. Cowley, B. Moran, M. Rice, "Cramer-Rao lower bounds for QAM phase and frequency estimation," IEEE Trans. Commun., vol. 49, pp 1582-1591, Sep. 2001

[6] N. Noels, H. Steendam and M. Moeneclaey, "The Impact of the Observation Model on the Cramer-Rao Bound for Carrier and Frequency Synchronization", in Proc. IEEE Int. Conf. Communications 2003, Anchorage, Alaska, Paper CT04-1, May 2003

[7] N. Noels, H. Steendam and M. Moeneclaey, "The true Cramer-Rao bound for timing recovery from a bandlimited linearly modulated waveform," in Proc. IEEE Int. Conf. Communications 2002, New York, Paper D08-1, April 2002

[8] N. Noels, H. Steendam and M. Moeneclaey, "The Cramer-Rao Bound for Phase Estimation from Coded Linearly Modulated Signals," accepted for publication in IEEE Comm Letters.

[9] M. Moeneclaey, "On the true and modified Cramer-Rao bounds for the estimation of a scalar parameter in the presence of nuisance parameters," IEEE Trans. Comm., vol COM-46, pp. 1536-1544, Nov. 1998.

[10] L.R. Bahl, J. Cocke, F. Jelinek and J. Raviv, "Optimal decoding of linear codes for minimizing symbol error rate," IEEE Trans. Inform. Theory, vol IT-20, pp. 248-287, March 1974.

[11] C. Berrou and A. Glavieux, "Near Optimum Error correcting Coding and Decoding: Turbo codes," IEEE Trans. Commun., vol. 44, pp 1261-1271, Oct. 1996

[12] T. Richardson, "The geometry of turbo-decoding dynamics," IEEE Trans. Inf. Theory, vol. 46, pp 9-23, Jan 2000

[13] A. D'Amico, A.N. D'Andrea and R. Reggiannini, "Efficient Non-Data-Aided Carrier and Clock Recovery for Satellite DVB at Very Low Signal-to-Noise Ratios," IEEE Journal on selected areas in communications, vol. 19, No. 12, pp. 2320-2330, Dec. 2001

[14] D.C. Rife and R.R. Boorstyn, " Single tone parameter estimation from discrete-time observations," IEEE Trans. Inform. Theory, vol. IT-20, pp. 591-598, Sept. 1974

[15] B. Beahan, "Frequency Estimation of Partitioned Reference Symbol Sequences," Master Thesis, University of South Australia, April 2001, available at www.itr.unisa.edu.au/rd/pubs/thesis/theses.html

[16] N. Noels et Al., "Turbo Synchronization: an EM algorithm interpretation," in Proc. IEEE Int. Conf. Comm. 2003, Anchorage, Alaska, Paper CT22-2, May 2003.

[17] R.A. Boyles, "On the convergence of the EM algorithm," J.R.Statist. Soc. B, 45, No. 1, pp.47-50, 1983

[18] J.A. Gansman, J.V. Krogmeier and M.P. Fitz, "Single Frequency Estimation with Non-Uniform Sampling," in Proc. of the 13th Asilomar Conference on Signals, Systems and Computers, Pacific Grove, CA, pp.878-882, Nov. 1996

[19] C. Herzet, V. Ramon, L.Vandendorpe and M. Moeneclaey, "EM algorithm-based timing synchronization in turbo receivers," in Proc. ICASSP 2003, Hong Kong, April 2003

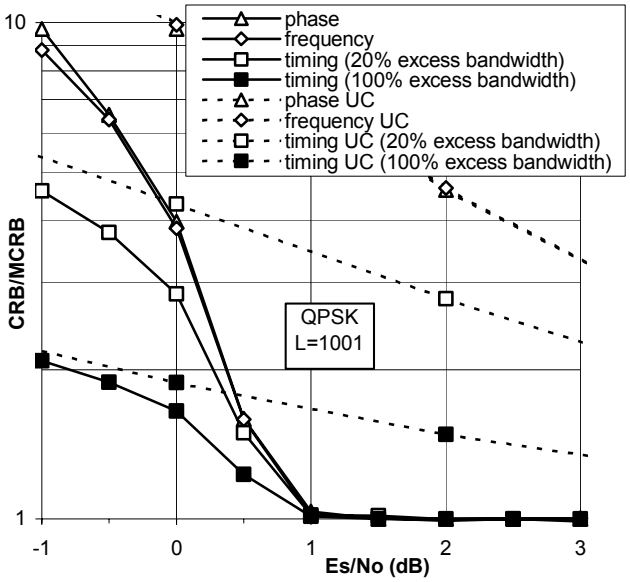

Fig.1: Comparison of the ratio CRB/MCRB for turbo encoded transmission with the ratio CRB/MCRB for uncoded (UC) transmission; for QPSK symbols and an observation length L=1001

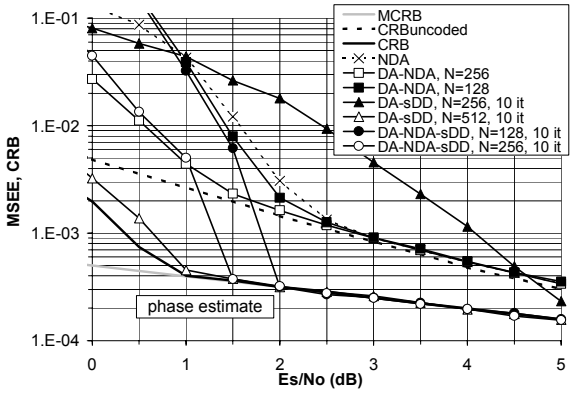

Fig.2: Comparison of the MSEE of practical estimators with the CRB (phase estimate)

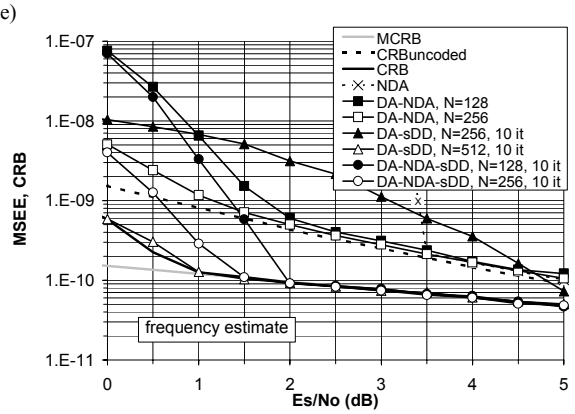

Fig.3: Comparison of the MSEE of practical estimators with the CRB (frequency estimate)